

Using Total Internal Reflection Fluorescence Microscopy, DNA Curtains, and Quantum Dots to Investigate Protein-DNA Interactions at the Single-molecule Level

M-L. Visnapuu, D. Duzdevich and Eric C. Greene*

Department of Biochemistry and Molecular Biophysics, Columbia University, 650 West 168th Street, Black Building Room 536, New York, NY 10032, USA

Recent years have witnessed an explosion of microscopy techniques that enable the experimental observation of individual biochemical reactions, and these new methods have opened up an entirely new field of scientific investigation. Total internal reflection fluorescence microscopy (TIRFM) is one example of a new experimental tool being employed to visualize biology at the molecular level, and is particularly well-suited for studying the interactions between proteins and nucleic acids. Yet these experiments are technically demanding, the observation times are limited by the photostability of the fluorescent reagents used to label the samples, and it is often difficult and time-consuming to obtain statistically relevant information. However, advances in surface engineering techniques combined with newly developed fluorescent labeling reagents have now made it possible to simultaneously monitor hundreds of individual protein-DNA interactions in real time with TIRFM, facilitating single-molecule experimentation with the promise of further scientific breakthroughs.

Keywords single molecule microscopy; TIRFM; lipid bilayer; DNA curtain; protein-DNA interactions; quantum dots

"I've spent more time than many will believe [making microscopic observations], but I've done them with joy, and I've taken no notice of those who have said why take so much trouble and what good is it?"

-Antonie van Leeuwenhoek (1632-1723)

1. Introduction

Advances in biology are often made possible through the development of new technologies. For example, the pioneering efforts of several research groups have advanced microscopy to the point where it is now possible to visualize individual biological molecules as they perform their functions in real time. These newly emerging technologies are already beginning to revolutionize the ways that we think about and approach biochemistry and molecular biology. The study of the interactions between proteins and nucleic acids is one area of biological research in particular that stands to benefit from these recent advances.

Many aspects of DNA metabolism are dependent upon the interactions between proteins and DNA. This includes DNA replication and chromosome segregation, DNA repair and maintenance, and the regulation of gene expression. Defects in any of these processes can lead to devastating consequences for the cell and also directly affect human health. In fact, most cancers and other genetic diseases are the result of mutations or other abnormalities that impact some aspect of DNA metabolism [1-4]. Because of their obvious importance, protein-DNA interactions have been a major subject of experimental investigation in molecular biology and biochemistry, and as a consequence we now understand many of the underlying principles that enable DNA-binding proteins to fulfill their biological roles. However, traditional experimental approaches that rely upon measurements of bulk populations of molecules are often hampered by an inability to elucidate crucial details of reaction dynamics. Similarly, bulk studies often fail to resolve rare or transient intermediates because they can only yield population averaged

* Corresponding author: ecg2108@columbia.edu

measurements. Many of these previous impediments can now be overcome through the use of specialized optical microscopy methods that complement more traditional biochemical approaches by enabling the visual detection of individual protein and DNA molecules under conditions that do not perturb their biological properties. Moreover, single-molecule experiments allow for quantitative probing of individual reaction trajectories and enable one to monitor reaction pathways or subpopulations of molecules that would be impossible to detect with traditional bulk studies. These new optical microscopy methods have already demonstrated potential by enabling exciting new scientific breakthroughs that were simply not possible with previously existing technologies.

2. Overview of TIRFM

Total internal reflection fluorescence microscopy (TIRFM) has emerged as an extremely powerful tool that can be used to study dynamic aspects of individual biochemical reactions in real-time using non-invasive detection methods. TIRFM makes use of an interesting property of light that is reflected at an interface between two transparent materials of differing refractive indexes [5-6]. For TIRFM, a laser beam is directed through a microscope slide and reflected off the interface between the slide and an aqueous buffer. If the angle of incidence is greater than the critical angle:

$$\theta_c = \sin^{-1}\left(n_1 / n_2\right)$$

(where n_1 and n_2 are the refractive indexes of the buffer and slide, respectively) then the beam is reflected away from the interface. However, the light does not reflect abruptly; an illuminated region, called the evanescent wave, is present on the sample side of the slide and its intensity decays exponentially away from the interface. The physical explanation for this phenomenon is that the electrical and magnetic wave components of the incident photons can not be discontinuous at the interface, therefore upon reflection some of the energy must penetrate beyond the boundary between the two media. For most applications, the evanescent wave penetrates only 100-300 nanometers (nm) into the aqueous medium and its intensity (I) at a given depth (z) can be calculated as:

$$I(z) = I(0)e^{-z/d}$$

where:

$$d = \frac{\lambda}{4\pi}\left[n_2^2 \sin^2\theta - n_1^2\right]^{1/2}$$

(and λ is the wavelength of the light impinging on the interface at angle θ). This yields a very small excitation volume–typically on the order of just a few femptoliters (~10^{-15} liters). The significance of this illumination configuration is that it greatly reduces the background signal typically associated with wide-field epifluorescence illumination by selectively exciting only the fluorescent molecules that reside within a very small volume located near the interface between the two transparent media. This spatially selective excitation allows for the observation of single fluorescently labeled molecules because only molecules very close to the slide surface are illuminated. Contaminants and molecules in bulk solution do not contribute to the detected signal, thereby reducing the background noise by several orders of magnitude relative to conventional wide-field illumination techniques (Figure 1). This in turn enables detection of subpopulations within a heterogeneous mixture of biological molecules and can be used to identify transient intermediates along a reaction trajectory. For additional discussion of more detailed aspects of TIRFM theory we refer the reader to several excellent reviews [5-6].

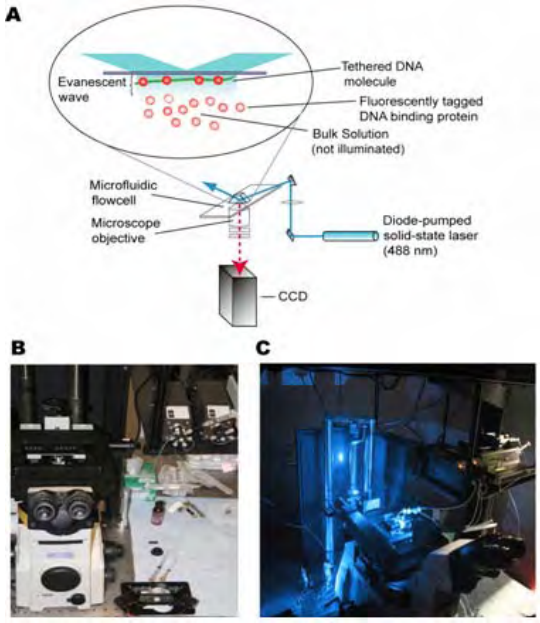

Fig. 1 TIRFM Microscope. (A) Our systems are custom built around Nikon TE2000U inverted microscopes and each is equipped with a 100x oil immersion lens. The laser illumination wavelength depends upon the fluorophores utilized in a given experiment; for studies involving quantum dots we use a 488nm, 200 mW diode-pumped solid-state laser (Sapphire-CDHR; Coherent, Inc.). The beam is focused through a fused silica prism onto the slide surface, creating the evanescent field. Light emitted by the fluorophores is collected with a CCD camera (Photometrics, Cascade 512B); for two color experiments, an image splitter (Dual-View; Roper Bioscience) separates the emission spectra of quantum dots emitting at different wavelengths and focuses each image onto a separate half of the EMCCD detector. The resulting images are later digitally recombined using image-processing software. (B) The objective is visible with the stage removed: note the flowcell is mounted in place on the removable stage (also see Figure 2). (C) The laser beam is guided to the prism face with a remotely operated mirror (New Focus) that can precisely control the location of the illumination field relative to the objective underneath.

Daniel Axelrod and colleagues pioneered the use of TIRFM as an experimental tool to study biological membranes [5-6], but these early TIRFM experiments were not yet able to resolve individual molecules. The use of TIRFM for visualizing single fluorescent molecules was brought about through significant advances in charge-coupled device (CCD) technologies that greatly enhanced the ability of these cameras to detect very faint signals. Most of these early CCD cameras relied upon signal intensifiers that were essentially the equivalent of military night-vision goggles, which when combined with high quantum efficiency image sensors allowed for single photon detection. Some newer cameras use back-illuminated CCDs with on-chip signal amplification and can achieve ≥90% detection efficiency across the visible spectrum. In addition to better cameras, single-molecule studies have benefited greatly from improved fluorophores, as well as rigorous preparation of materials and hardware to eliminate all possible sources of background signal. Many of these advances were made possible through the pioneering efforts of Toshio Yanagida and colleagues in the early to mid 1990's. The culmination of these technical achievements led to many seminal studies of biological systems, including the imaging of ATP turnover by single molecules of myosin [7], visualization of single molecules of GFP (green fluorescent protein) and the revelation that they cycle between bright and dark states [8], quantification of the folding and catalysis of single RNA molecules [9], visualization of DNA unwinding by individual molecules of Rep helicase [10], observation of myosin molecules as they walk along actin filaments [11], and the detection of intermediate states during protein translation by single ribosomes [12]. These experiments utilized TIRFM to study individual molecules and would not have been possible through ensemble averaged experimental methods.

3. Instrumentation

TIRFM systems are now commercially available from several sources, but they can also be assembled using off-the-shelf components. The primary advantage of home-built systems is that they are easily modified to accommodate a wide range of experimental requirements. Our laboratory uses a custom-made TIRFM setup, which is built around a Nikon TE2000U microscope and relies on a simple through-prism illumination configuration (Figure 1). The excitation source is provided by the beam from a diode-pumped solid-state laser (DPSSL; 488 nm, 200 mW, Sapphire, Coherent, Inc.), which is focused through

the face of a fused silica prism onto a microfluidic flowcell ($\theta_c \approx 65°$ for the interface formed by fused silica and water) to generate an evanescent wave within the sample chamber. Coarse alignment of the beam is achieved by visual inspection of its position relative to the front lens of the objective. Fine alignment is controlled by a remotely operated motorized mirror (New Focus, Inc.) that guides the beam to the prism face. Photons are collected with a microscope objective (100X, 1.4 NA, oil immersion Plan Apo, Nikon), passed through a notch filter (Semrock) to reject scattered laser light, and detected using a back-illuminated electron-multiplying CCD (EMCCD; Cascade II, Photometrics). Similarly suitable cameras are also available from other manufacturers. When used for multi-color operation, the photons are passed through an image-splitter (Roper Bioscience) containing a dichroic mirror that separates the optical paths. Each image is focused onto a separate half of the EMCCD to allow simultaneous dual-color imaging. The entire TIRFM system is mounted on an optical table (Newport Corp.) to minimize vibrations and to facilitate alignment of optical components. Such TIRFM systems are capable of detecting single fluorophores with millisecond temporal resolution and can be used for single-pair fluorescence resonance energy transfer (spFRET) [13], co-localization of reaction components, multi-color detection, and single particle tracking [14-15].

All of our single-molecule TIRFM experiments are performed within microfluidic flowcells that are machined and assembled in house. The flowcell provides a sample chamber within which reactions can be precisely controlled, and thus allows for the observation of individual biomolecules under a broad range of conditions. Each flowcell is made from a 76.2 x 25.4 x 1 mm fused silica glass slide (ESCO Products, Inc.). Conventional borosilicate slides are not recommended because they contribute to background noise and significantly compromise signal detection. To begin assembly, inlet and outlet holes are bored into each slide using a diamond-coated 1.4 mm drill bit (Eurotool) mounted on a high-precision drill press (Servo Products Company). To minimize damage to the slide surface during the drilling procedure and ensure smooth boring, the slide is placed atop a simple plastic mount and then submerged under continuously flowing water, which cools the slide and washes away fused silica dust during drilling (Figure 2). Slides are then thoroughly cleaned by sequential submersion in 10% HELLMANEX™, 1M NaOH (for 30 minutes each), and MilliQ™ water (3 x 15 minutes) and the slides are rinsed under running MilliQ™ water between each step. This is followed by a rinse in absolute methanol and drying at 120°C under vacuum for at least one hour. Micro-scale diffusion barriers (see below) are etched onto the surface using a diamond-coated scribe [16]. The sample chamber is prepared by excision of a channel on double-sided tape (3M) placed over the slide, which is then overlaid with a borosilicate glass coverslip (Fisher Scientific). Inlet and outlet ports (Upchurch Scientific) are attached with adhesive rings over the drilled holes (Figure 2). The assembled flowcell is clamped between two additional slides to evenly distribute pressure and placed in a 120°C vacuum oven for two hours to cure. Before beginning an experiment the completed flowcell is mounted in a custom-designed, microprocessor-controlled heating unit that is used to maintain the sample at any desired temperature (Figure 2). The entire assembly is mounted on a remotely operated stage (Ludl Electronic Products Ltd.) enabling the user to rapidly scan and select different fields. A syringe pump (KD Scientific) is connected to the flowcell to precisely control the rate of buffer flow through the chamber, and an HPLC 6-way injection valve (SCIVEX) is utilized to deliver samples. Flowcells are not recycled because surface quality decreases substantially following each use; the Nanoports however can be removed from the flowcell with methanol and reused indefinitely.

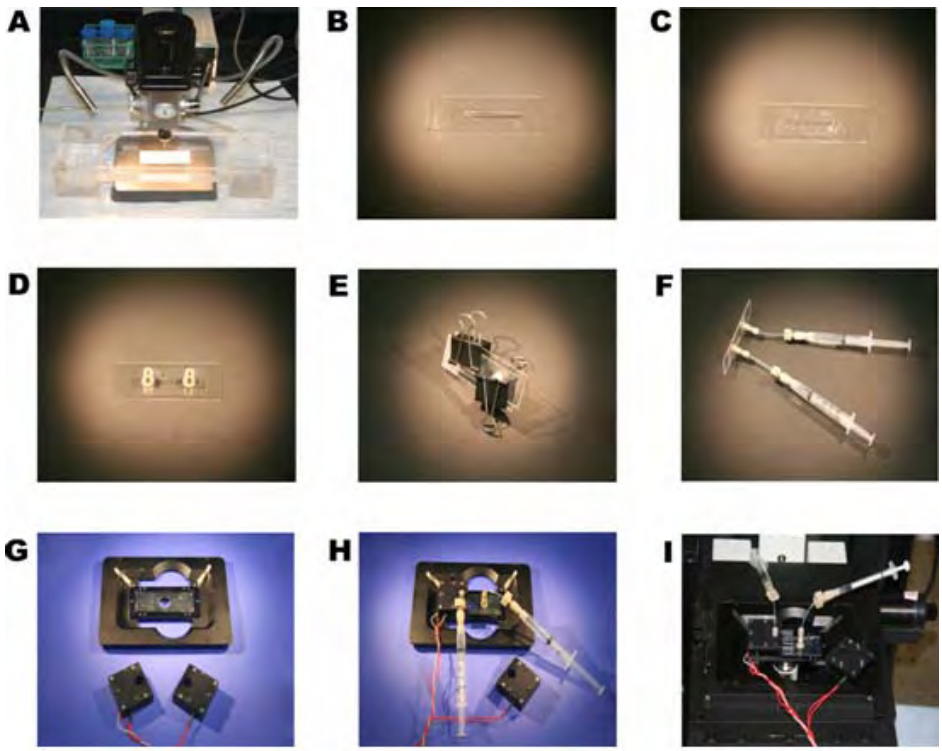

Fig. 2 Flowcell construction. (A) Two holes are bored into the fused silica glass slide with a precision drill press while immersed in a continuously flowing water bath to wash away glass dust. (B) After a thorough cleaning procedure, the slide is covered with double-sided tape. (C) A narrow channel is excised which is then covered by a glass coverslip. (D) Nanoports are attached with adhesive rings; the slide is clamped (E) and placed in a vacuum oven to seal the chamber. (F) The lipid vesicles, neutravidin and DNA are manually delivered using syringes attached to the nanoports. When a flowcell is ready for use, it is placed on the microscope stage and held in place by heating units as shown in (G), (H) and (I). Note the prism on top of the flowcell and the objective underneath in (I).

4. DNA Curtains and "High-throughput" Single-molecule Microscopy

Despite the obvious benefits, TIRFM does suffer from two potential problems that can limit its broader applicability. First, the unique illumination geometry of TIRFM enables detection of single fluorophores, but also requires that molecules under study be tethered to a solid surface to ensure that they remain confined within the excitation volume defined by the penetration depth of the evanescent field for the duration of the observation. Therefore, it is absolutely essential to use surfaces that minimize nonspecific interactions with the biomolecules under investigation yet can provide solid attachment points that do not comprise the biological integrity of the sample. In addition, it is inherently difficult to collect statistically relevant information from experiments designed to probe one reaction at a time, and this difficulty can be compounded by the use of large DNA molecules, which are the primary substrates used for our studies. This means that it can often take long periods of time to optimize any given experimental system and collect enough data to allow reasonable interpretation of the results.

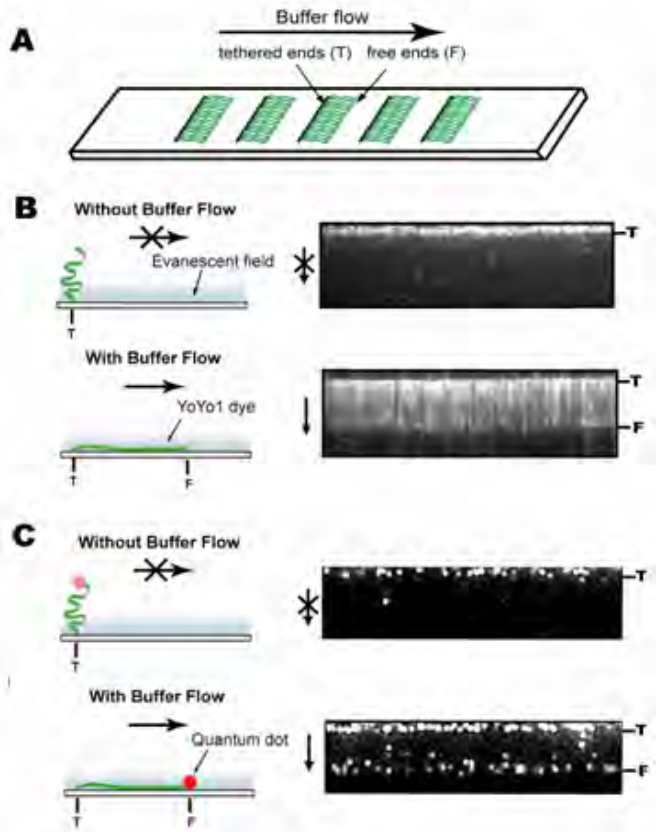

Fig. 3 DNA curtain assay. DNA curtains allow for the visualization of hundreds of DNA and protein molecules in a single field-of-view. (A) Buffer flow pushes the DNA molecules (shown in green) that are tethered to the fluid lipid bilayer up to the leading edge of a microscale diffusion, this leads to formation of a "DNA curtain". (B) The flow extends the labeled DNA molecules into the evanescent field allowing for the visualization of the molecules. In the absence of flow the DNA molecules diffuse away from the surface and only the tethered ends remain visible. A sample DNA curtain stained with fluorescent YOYO1 dye is shown on the right. A diagram and a DNA curtain where the ends of the molecules are labeled with fluorescent quantum dots is shown in (C). Both sample DNA curtains are shown with (top panel) and without (bottom panel) buffer flow. "T" and "F" mark the tethered and free ends of the molecules, respectively.

To help overcome both of these problems we have developed a new technology referred to as "DNA curtains," which enables the simultaneous detection of up to hundreds of individual DNA molecules within a single field-of-view [14-17]. All of the DNA molecules within the curtain are physically aligned with respect to one another and are located at defined positions on the surface of the sample chamber. The surface itself is coated with a fluid lipid bilayer, which renders it inert and prevents any molecules from adhering to the fused silica. Complete details of procedures for preparing the DNA curtains have been presented elsewhere [16]. In brief, the surface of the slide is manually etched with a diamond-coated drill bit prior to the assembly of the flowcell, as described above, yielding microscale lipid diffusion barriers perpendicular to the direction in which the buffer will flow during the experiment. The surface of the microfluidic sample chamber is then coated with a supported lipid bilayer. The bilayer is prepared by injecting lipid vesicles (Avanti Polar Lipids, Inc.) comprised of a mixture of DOPC (1,2-dioleoyl-*sn*-glycero-phosphocholine), 0.5% biotinylated-DPPE (1,2-dipalmitoyl-*sn*-glycero-3-phosphoethanolamine-N-(cap biotinyl)), and 8-10% mPEG 2000-PE (1,2-dioleoyl-*sn*-glycero-3-phosphoethanolamine-N-[methoxy(polyethylene glycol)-2000]) into the sample chambers. The vesicles spontaneously rupture on the surface and self-assemble into a planar bilayer separated from the fused silica by a water layer approximately 1-2 nm thick. After the bilayer has formed the excess vesicles are removed by flushing the chamber with fresh buffer. Neutravidin (Pierce Biotechnology, Inc.) is then applied to the bilayer surface and acts as a multivalent linker between the biotinylated-DPPE and any biotinylated DNA molecules that are subsequently injected into the chamber. Most of our experiments utilize λ-DNA (48,502 base pairs, ~16 μm in length; Invitrogen), which is biotinylated at one end with a tagged oligonucleotide complementary to the 12-nucleotide ssDNA overhang present at the ends of the linear λ-DNA. This tethering strategy yields DNA molecules that are anchored by one end to the bilayer through an interaction with a single lipid. For visual detection the DNA molecules can be labeled with

either a fluorescent interchelating dye such as YOYO-1 (Invitrogen) [14], or they can be labeled at their free ends with single quantum dots [18] (see below and Figure 3).

The bilayer serves two important purposes: (1) it renders the surface inert by providing a microenvironment that closely mimics natural cell membranes [19], and (2) it permits the end-tethered DNA molecules to move in two dimensions while confining them near the sample chamber surface [16]. Importantly, the microscale diffusion barriers etched into the flowcell surface cannot be traversed by the lipids [20]. Therefore when buffer flow is applied to the sample chamber the lipid-tethered DNA molecules are driven in the direction of flow and accumulate at the leading edges of the diffusion barriers. Application of the hydrodynamic force also extends the DNA molecules parallel to the sample chamber surface and confines them within the detection volume defined by the penetration depth of the evanescent field. Transiently pausing the buffer flow causes the DNA molecules to briefly diffuse out of the evanescent field, but any molecules that are nonspecifically stuck to the surface remain within view and can be discounted from further analysis (Figure 3). This simple, but essential control can be used to verify that any sample under observation is not nonspecifically stuck to the sample chamber surface.

Thousands of DNA molecules can be aligned at a given microscale diffusion barrier, and the density of the DNA can be varied to suit any specific experimental requirements [16]. This is achieved by simply increasing or decreasing the amount of DNA that is injected into the sample chamber or alternatively by varying the distance between adjacent barriers on the surface. These DNA curtains allow for the visualization of hundreds of individual DNA molecules within a single field-of-view, and greatly increase the throughput capacity of the TIRFM single-molecule experiments. Data analysis is also simplified because all of the DNA molecules are physically aligned with respect to one another, enabling straightforward molecule-to-molecule comparisons.

5. Quantum Dots as Labels for Single-molecule Studies

An important aspect of many biological problems is that the underlying biochemical reactions can often occur on timescales that span several minutes or even longer. Under the intense laser illumination required for TIRFM, traditional fluorophores such as Cy3 or GFP (green fluorescent protein) photobleach within just seconds. To overcome this limitation most of our work now relies on fluorescent semiconducting nanocrystals as the fluorophore of choice rather than other types of fluorescent dyes (Figure 4). Fluorescent semiconducting nanocrystals, also called quantum dots or Qdots, are a revolutionarily new type of fluorescent label that offers many significant advantages over traditional organic fluorophores. Semiconducting nanocrystals were originally of great interest in the field of quantum physics because their very unusual physical properties allow them to function essentially as “artificial atoms” [21]. It was found that excitation of these crystals with light of the appropriate wavelength results in an electron-hole pair (referred to as an exciton); when the pair recombines a photon is emitted at a longer wavelength and the nanocrystals fluoresce [22-23]. Chemical studies continued to reveal the physical properties of semiconducting nanocrystals [23-24], which in turn paved the way for broader applications. It was quickly recognized that their use for biological studies would require several modifications to the naked crystals. In particular, early quantum dots were only soluble in organic solvents, they did not have uniform fluorescent properties, and there were no available chemistries for gently attaching them to biological molecules such as proteins or DNA. Part of the solution came in the form of a protective outer shell of zinc sulfide (ZnS) around the semiconductor core, which mitigates the effects of any crystalline imperfections on the core surface. Further advances led to quantum dots that are coated with a final outer layer of hydrophilic material, such as mercaptoacetic acid or polyethylene glycol [26-28], which is necessary to ensure water solubility and also adds the functional groups required for convenient coupling to proteins.

By the late 1990's many novel uses of quantum dots in biology had been realized, and they have since been applied to immunofluorescence studies of fixed tissues, in vivo fluorescence assays, as well as in vitro biochemical studies [23, 28, 31]. Biotechnology companies now offer Qdots engineered specifically for biological applications, making them an even more attractive option for single-molecule microscopy. Most commercially available quantum dots that emit within the visible spectrum are made of either a

cadmium selenide (CdSe) or cadmium telluride (CdTe) core surrounded by a ZnS shell. They are relatively small (typically ranging from 2-20 nanometers in diameter) with the size of the Qdot corresponding to its emission spectrum (a larger diameter translates into emission of longer wavelength light). Because their size can be precisely controlled during synthesis [29-30], so can their emission color (Figure 4). Quantum dots are extremely bright – up to 100-fold brighter than most other fluorophores – making them extremely easy to detect. They are also highly photostable, which means that they do not photobleach on timescales relevant to biological studies. Quantum dots also have large absorptive cross-sections (with extinction coefficients often exceeding $1x10^6$ $M^{-1}cm^{-1}$), broad excitation peaks, and narrow emission bands. In practical terms this means that a single laser source can be used to excite quantum dots that emit in many different regions of the visible spectrum, eliminating the need for multiple illumination sources during applications requiring multi-color imaging.

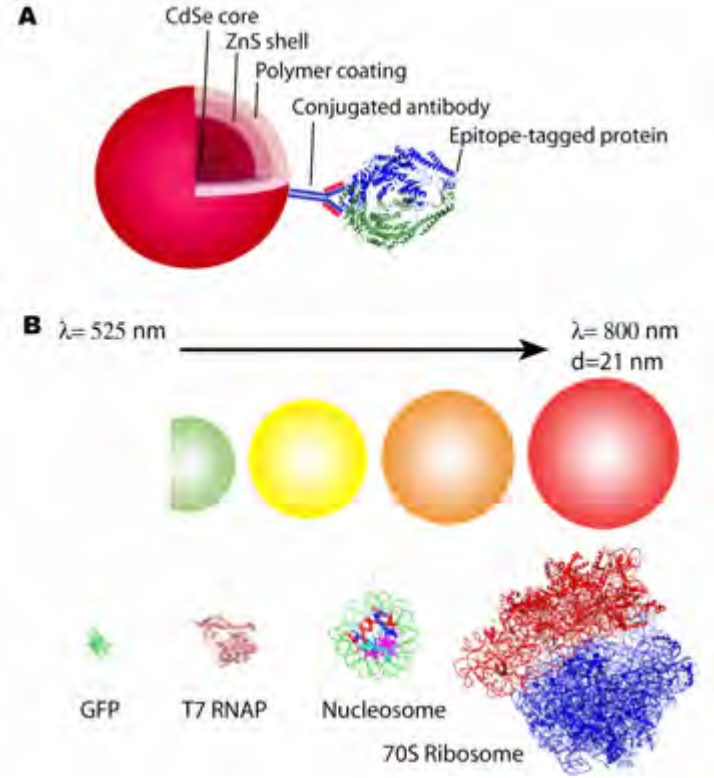

Fig. 4 Quantum dots can be used for labeling proteins and DNA in single molecule assays. (A) Quantum dots contain a CdSe or CdTe core, a ZnS shell and a polymer coating such as polyethylene glycol. Antibodies against a wide range of epitope tags can be conjugated to the coating of the quantum dot to allow for the labeling of any protein of interest with the appropriate tag. The size of the core of the quantum dot determines the emission color of the particle; most commercially available quantum dot emission wavelengths range from 500-800 nm. (C) The Qdots in this color range are 10-20 nm in diameter, roughly the size of single proteins and small protein complexes [38-42]. The depictions of the quantum dots and the proteins are to scale so as to illustrate their realative sizes.

Most of our current experiments utilize a labeling strategy in which recombinant proteins are expressed as fusions with an epitope tag (e.g. HA, FLAG, thioredoxin, etc.) and these tags are used as handles for conjugating the protein of interest to a quantum dot that is covalently coupled to the corresponding antibody [15, 32]. We primarily work with quantum dots that are coated with short-chained polyethelyne glycol, and a subset of these polymers terminate in a primary amine (Invitrogen). The free amines on the outer surface of the quantum dots can be labeled with affinity purified, reduced antibodies using the hetero-bifunctional crosslinking reagent SMCC (succinimidyl 4-[N-maleimidomethyl]cyclohexane-1-carboxylate). According to the manufacturer this procedure yields on the order of 1-3 antibodies per quantum dot, and this value is also consistent with our own analytical gel filtration analysis. The resulting quantum dot antibody conjugates can be purified by gel filtration to remove any unreacted antibodies and stored in PBS (pH 7.4) at 4 C for at least several weeks without a noticeable decline in quality. The antibody labeled quantum dots can then easily be coupled to the epitope-tagged recombinant protein of interest.

As an added advantage this labeling strategy can be applied to virtually any protein that has an epitope tag and is unaffected by the attachment of the Qdot. It is notable that most *S. cerevisiae* proteins have already been expressed with bulky epitope tags without affecting the viability of the organism [33-34], suggesting that many proteins may retain function when linked to a quantum dot. Nevertheless, this tagging strategy may not be applicable for all studies and it is critical to assess the effect of the epitope tag and bound quantum dot for any protein under investigation through the use of standard in vitro ensemble assays. This is necessary to ensure that the biochemical properties of the proteins under investigation are not altered by the labeling procedure.

6. Data Collection, Analysis, and What can be Learned

Once suitably labeled proteins have been prepared they are injected into a sample chamber containing a DNA curtain and their behavior can be monitored in real time by visualizing the reactions with TIRFM. Reaction conditions and details of the data collection depend primarily upon the biochemical properties of the system under investigation and the questions that are being addressed (for additional details please refer to any of the following: [14-15, 32]). In our systems, data acquisition is performed with a PC

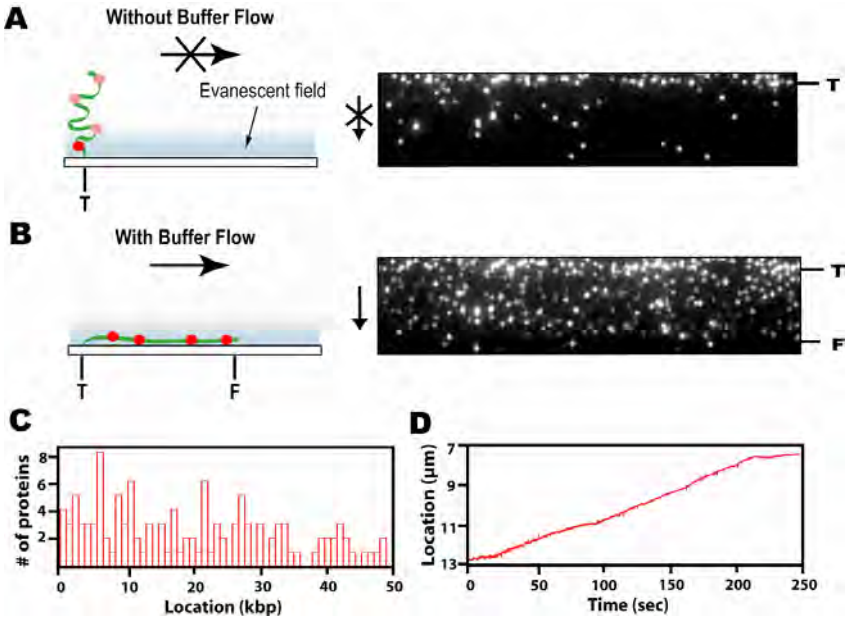

Fig. 5 Visualizing protein-DNA interactions. Fluorescently labeled proteins can be visualized when bound to DNA molecules as buffer flow extends the DNA into the evanescent field. (A) Rdh54 is bound to DNA curtains [15]. The protein is labeled with quantum dots while the DNA is unlabeled. (B) Buffer flow extends the DNA, allowing for the visualization of the labeled Rdh54. (C) The curtain setup allows us to investigate whether the proteins display any regional or site-specific DNA binding preferences. We can study the distribution of binding sites of fluorescent proteins on hundreds of DNA molecules by defining particles and their positions using Igor Pro software. (D) A sample track of a translocating Rdh54 complex is shown (refer to [15] for additional information).

running NIS-Elements software (Nikon), and the resulting image files are saved to a hard drive. After data collection, all image analysis is done using custom algorithms written in NIH ImageJ (available at http://rsb.info.nih.gov/ij/) or Igor Pro (WaveMetrics) and full details of these procedures have been published [15, 32]. One of the first analytical procedures conducted is to count fluorescent particles and determine their position distribution on the DNA curtain (Figure 5) [15]. This is used to determine whether the protein displays any regional or site-specific DNA binding preferences or whether it binds randomly along the DNA [15]. The position of each individual protein can be followed over time using a

particle-tracking algorithm that follows the movements of each fluorescently tagged protein by fitting the successive images within a video to a 2D Gaussian function (Figure 5) [15]. The particle-tracking data allows us to quantify the behavior of an individual Qdot over time and/or in response to changes in reaction conditions (Figure 6). For example, it is possible to quantify the behavior of proteins that travel along the DNA molecules [15].

Using TIRFM we have visualized the behavior of the molecular motor Rdh54, which is an Snf2 protein involved in homologous DNA recombination [15]. Homologous recombination is necessary to repair double-stranded DNA breaks, one of the most dangerous forms of DNA damage, and is also an essential pathway for generating genetic diversity during meiosis [35]. We have shown that Rdh54 binds randomly to DNA molecules and can actively translocate along the DNA using the energy derived from the hydrolysis of ATP as its fuel source. Rdh54 moves at a mean velocity of approximately 80 base pairs per second, generates large loops in the DNA molecules as it travels along the double helix, and the complexes can spontaneously stop and reverse direction. We have now been able to provide a quantitative assessment of these motor functions, which would not have been possible using standard

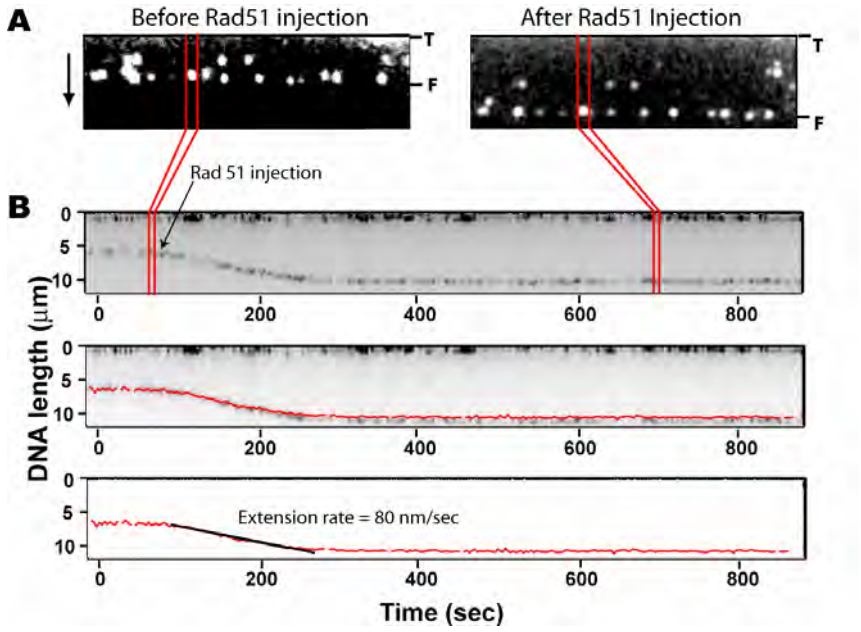

Fig. 6. Quantifying protein behavior. The position of Qdot bound either to protein or DNA can be followed over time by using a particle-tracking algorithm. In (A), the ends of the DNA molecules are labeled with Qdot. The panel on the left shows the DNA curtain right before Rad51 is injected into the flowcell. The panel on the right illustrates Rad51 extending the DNA molecules as indicated by the new position of the Qdot labeled free end. An image slice containing a single DNA molecule is shown over time in a kymogram in the top panel of (B). The tracking data is overlaid with the kymogram in the middle panel and the tracking data is presented in the bottom panel. This allows us to quantify the behavior of an individual Qdot over time by fitting the appropriate mathematical functions to the tracking curves. The extension curve of DNA by Rad51 can be fit by a least-squares linear function and the extension rate can be determined (bottom panel, B).

biochemical techniques. Rad51 is another essential protein that is required for homologous DNA recombination: it forms an extended nucleoprotein filament along DNA. The DNA within this filament is stretched by approximately 50% relative to normal B-DNA and this DNA extension provides a convenient signal that can be used to monitor nucleoprotein filament assembly and disassembly in real time by TIRFM [14, 18]. In addition, we have shown that some forms of Rad51 are capable of sliding

along the DNA molecules [17]. These ongoing investigations promise to yield new information regarding the interactions between these nucleoprotein filaments and other proteins that are critical for homologous recombination.

We have also begun to probe the mechanisms of post-replicative mismatch repair (MMR) protein complex Msh2-Msh6, which is a damage sensing protein responsible for detecting and initiating the repair of mispaired bases that occur as a consequence of errors during DNA replication [36]. Defects in MMR proteins lead to the most common forms of hereditary colon cancer, and many of these cases result from mutations in Msh2-Msh6 [37]. Despite this importance, it is still unclear precisely how MMR proteins function, but many of the remaining questions in the field concern how the various protein complexes travel along DNA at different stages of the repair reaction. In contrast to a molecular motor protein, we have found that Msh2-Msh6 travels passively along DNA by one-dimensional diffusion driven only by thermal energy [32]. Our data suggest a model in which Msh2-Msh6 rotates around the DNA by tracking the phosphate backbone as it slides back and forth scanning for mispaired bases. Moreover, this protein complex stops diffusing on the DNA at specific sites along the molecules which function as traps in the energy landscape and we speculate that these traps may mimic some aspects of a mispaired base. Interestingly, when given ATP the "trapped" molecules of Msh2-Msh6 can continue diffusing along the DNA molecules. This nucleotide exchange dependent escape from the traps may reflect mechanistic steps leading to the downstream events in the repair pathway; further studies are now under way to probe these steps in the pathway. A common aspect of each of these examples is that TIRFM allowed the systems to be studied in real time at the level of single biochemical reactions and the details revealed could not have been easily obtained with any other experimental technique.

7. Summary

Optical microscopy has been at the forefront of modern scientific research ever since Antonie van Leeuwenhoek used a simple magnifying lens to open biologist's eyes to the wonders of the microscopic world. Single-molecule research has provided yet another avenue of research perfectly suited to optical microscopy and these studies are now beginning to revolutionize the way that we think about and approach biological problems at the molecular level. This work combines aspects of physics, biochemistry, and micro-/nano-scale technology to answer important questions about biology that can not be addressed through traditional approaches. TIRFM, in particular, is uniquely adapted for studying protein-DNA interactions and can be used for probing reaction dynamics on time scales ranging from seconds to minutes or even longer. The benefits of TIRFM are that the experiments are done under solution conditions, there is no need for chemically fixing or otherwise inactivating the molecules being studied, and single proteins can be visualized on individual DNA molecules under a variety of different solution conditions in real time. This allows one to determine what proteins are bound to the DNA, where they are bound, when they dissociate, and how they affect one another. TIRFM still remains challenging, but as these techniques mature they will undoubtedly become less specialized. The introduction of inert lipid bilayers in the sample chambers and the development of DNA curtains combined with quantum dot-tagged proteins enables the rapid acquisition of statistically relevant information from hundreds of individual interactions, which should help make TIRFM a more powerful research tool. These novel research methods will greatly facilitate the use of TIRFM for studying a wide range of protein-DNA interactions and can be readily adapted to a variety of important biological systems.

Acknowledgements The authors thank members of the Greene laboratory for useful discussions and critical reading of the manuscript. We also thank Professor Louis E. Brus for an insightful discussion on quantum dots. The Greene laboratory is funded by research grants from the National Institutes of Health, the National Science Foundation, the March of Dimes, and the Susan G. Komen foundation.

References

[1] Hoeijmakers, J.H.J., *Nature* **411**, 366-374 (2001).
[2] Wood, R.D., et al., *Science* **291**, 1284-1289 (2001).
[3] Friedberg, E.C., *Nature* **421**, 436-440 (2003).
[4] Sjöblom, T., et al., *Science* **314**, 268-274 (2006).
[5] Axelrod, D., et al., *Annu. Rev. Biophys. Bioeng.* **13**, 247-268 (1984).
[6] Axelrod, D., *Methods in Cell Biol.* **30**, 245-270 (1989).
[7] Funatsu, T., et al., *Nature* **374**, 555-559 (1995).
[8] Dickson, R.M., et al., *Nature* **388**, 355-358 (1997).
[9] Zhuang, X., et al., *Science* **288**, 2048-2051 (2000).
[10] Ha, T., et al., *Nature* **419**, 638-641 (2002).
[11] Yildiz, A., et al., *Science* **300**, 2061-2065 (2003).
[12] Blanchard, S., et al., *Nat. Struct. Mol. Bio.* **11**, 1008-1014 (2004).
[13] Rasnik, I., et al., *Nat. Methods* **3**, 891-893 (2006).
[14] Prasad, T.K., et al., *JMB* **363**, 713-728 (2006).
[15] Prasad, T.K., et al., *JMB* (in press) (2007).
[16] Graneli, A., et al., *Langmuir* **22**, 292-299 (2005).
[17] Graneli, A., et al., *PNAS* **103**, 1221-1226 (2006).
[18] Robertson, R.B., et al., Disassemby kinetics of Rad51 nucleoprotein filaments. (Manuscript in preparation, 2007).
[19] Sackmann, E., *Science* **271**, 43-48 (1996).
[20] Groves, J.T., et al., *Acc. Chem. Res.* **35**, 149-157 (2002).
[21] Reed, M.A., et al., *Phys. Rev. Lett.* **60**, 535-537 (1988).
[22] Alivisatos, A.P., *Science* **271**, 933-937 (1996).
[23] Bruchez, M., et al., *Science* **281**, 2013-2016 (1998).
[24] Efros, Al. L., et al., *Sov. Phys. Semicond.* **16**, 772-775 (1982).
[25] Brus, L.E., *J. Chem. Phys.* **79**, 5566-5571 (1983).
[26] Chan, W.C.W., et al., *Science* **281**, 2016-2018 (1998).
[27] Larson, D.R., et al., *Science* **300**, 1434-1437 (2003).
[28] Medintz, I.L., et al., *Nat. Materials* **2**, 575-576 (2003).
[29] Murray, C.B., et al., *J. Am. Chem. Soc.* **115**, 8706-8715 (1993).
[30] Peng, X.G., et al., *J. Am Chem Soc.* **120**, 5343-5344 (1998).
[31] Michalet, F.F.P., et al., *Science* **307**, 538-544 (2005).
[32] Gorman, J., et al., Dynamic basis for one-dimensional DNA scanning by the mismatch repair complex Msh2-Msh6. (Submitted for publication, 2007).
[33] Krogan, N.J., et al., *Nature* **440**, 637-643 (2006).
[34] Huh, W.-K., et al., *Nature* **425**, 686-691 (2003).
[35] West, S.C., *Nat. Rev. Mol. Cell Biol.* **4**, 435-445 (2003).
[36] Kunkel, T.A., *Ann. Rev. Biochem.* **74**, 681-710 (2005).
[37] Modrich, P., *JBC* **281**, 30305-09 (2006).
[38] Yang, F., et al., *Nat. Biotechnology* **14**, 1246-1251 (1996).
[39] Junop, M.S., et al., *Mol. Cell* **7**, 1-12 (2001).
[40] Schuwirth, B.S., et al., *Nat. Struct. Mol. Bio.* **13**, 879-886 (2006).
[41] Luger, K., et al., *Nature* **389**, 251-260 (1997).
[42] Yin, Y.W., et al., *Cell* **116**, 393-404 (2004).